Observed Properties of Interstellar Dust[1]

1. **Wavelength-Dependent Extinction of Starlight**
2. **Polarization of Starlight**
3. **Scattering of Starlight**
4. **Total Volume of Interstellar Dust: The Purcell Limit**
5. **Asymptotic Behavior at Long Wavelengths**
6. **Abundance Constraints**
7. **Composition of Interstellar Dust**
8. **Far-Infrared Emission**
9. **Scattering of X-rays**
10. **Microwave Emission**
11. **Dust in Meteorites**

[1]N.B. This does not purport to be a review – citations are papers with which I happen to be familiar, and which should provide an entry point to the literature.

1. Wavelength-Dependent Extinction of Starlight

- Measured attenuation of starlight by interstellar dust

$$\tau_\lambda = \int n_d C_{\rm ext}(\lambda) ds \qquad (1)$$

  $C_{\rm ext}(\lambda)$ = extinction cross section
  n_d = number density of dust grains
  s = path length
  Astronomers measure attenuation in *magnitudes*:

$$\frac{A_\lambda}{\rm mag} \equiv 2.5\log_{10}\left[F_\lambda^0/F_\lambda\right] \qquad (2)$$

$$= 2.5\log_{10}\left[e^{\tau_\lambda}\right] = 1.086\,\tau_\lambda \qquad (3)$$

- Dust and gas are well-mixed: it is observed that $\tau_\lambda \propto N_{\rm H}$, where $N_{\rm H} \equiv \int n_{\rm H} ds$ is the column density of H nucleons
  Thus $n_d C_{\rm ext}/n_{\rm H} \approx const$

- Function A_λ = "the extinction curve".
  Because A_λ tends to be larger for shorter wavelengths, stars are "reddened" – hence we speak of "interstellar reddening".

- Because dust and gas appear to be well-mixed, and because H dominates the mass, it is natural to normalize to H: we discuss $A_\lambda/N_{\rm H}$.

How do we measure A_λ toward a given star?

1. Identify a nearby (unreddened) "twin" star (spectroscopic match)
2. Measure $F_\nu(\star)$ and $F_\nu(twin)$

$$F_\lambda = \frac{L_\lambda}{4\pi D^2} e^{-\tau_\lambda} \tag{4}$$

typo

$$\tau_\lambda(\star) - \tau_\lambda(twin) = \ln\left[\frac{F_\lambda(twin)}{F_\lambda(\star)}\right] + \ln\left[\frac{L_\lambda(\star)}{L_\lambda(twin)}\right] + \ln\left[\frac{D_\star^2}{D_{twin}^2}\right] \tag{5}$$

3. For nearby twin, can assume $\tau_\lambda(twin) \approx 0$, but generally don't know $(D_\star/D_{twin})$ (at least not accurately):
   Thus what we *really* measure is the "reddening curve":

$$\tau_{\lambda 1}(\star) - \tau_{\lambda 2}(\star) = \ln\left[\frac{F_{\lambda_1}(twin)}{F_{\lambda_1}(\star)}\right] - \ln\left[\frac{F_{\lambda_2}(twin)}{F_{\lambda_2}(\star)}\right] \tag{6}$$

   If $\lambda_2 \to \infty$, can assume $\tau_{\lambda_2} \approx 0$, and thereby measure absolute τ_{λ_1}.

4. Also measure $N_{\rm H}$ (e.g., using Lyα absorption line).
Plot $A_\lambda/N_{\rm H} = 1.086\tau_\lambda/N_{\rm H}$ for "average" sightline through diffuse ISM:

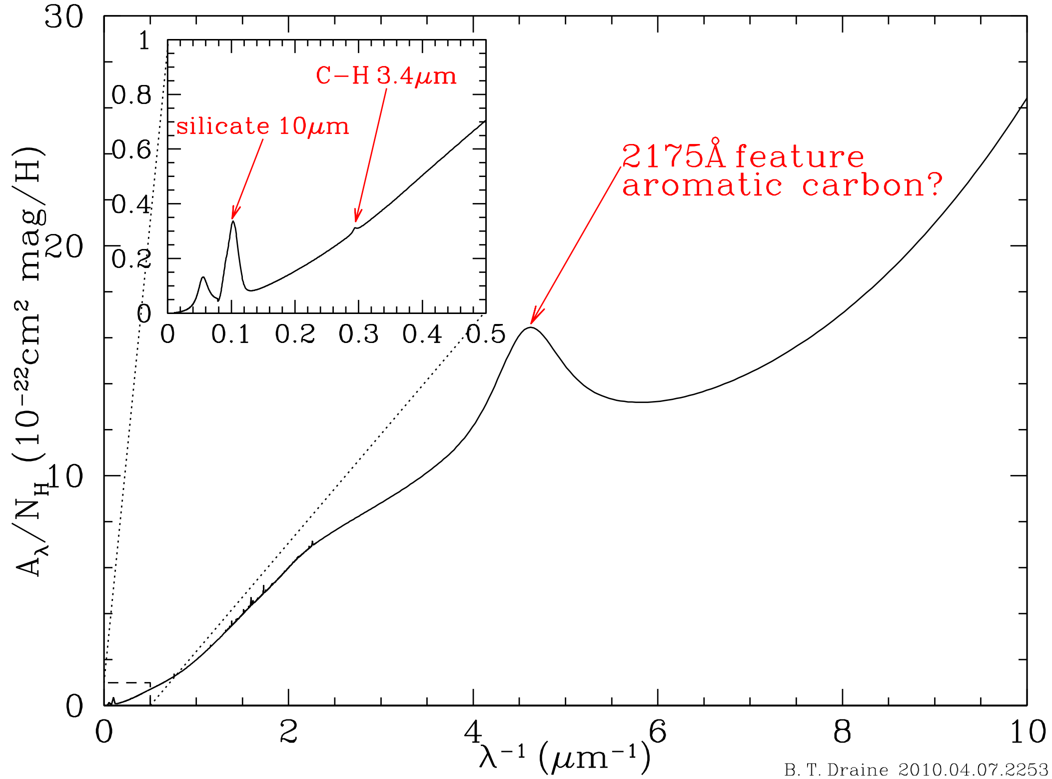

Principal features:

- General rise from IR to vacuum UV ($\sim 0.1\,\mu$m)
- $18\,\mu$m and $10\,\mu$m: O-Si-O bend and Si-0 stretch in amorphous silicates
- $3.4\,\mu$m: C-H stretch in hydrocarbons
- $0.2175\,\mu$m: "2200Å bump". Probably $\pi \rightarrow \pi^*$ electronic transition in sp^2-bonded carbon (e.g., graphite or PAH)
- $\gtrsim 400$ weak features – the *Diffuse Interstellar Bands* – still unidentified.

5. Variations seen among extinction curves:

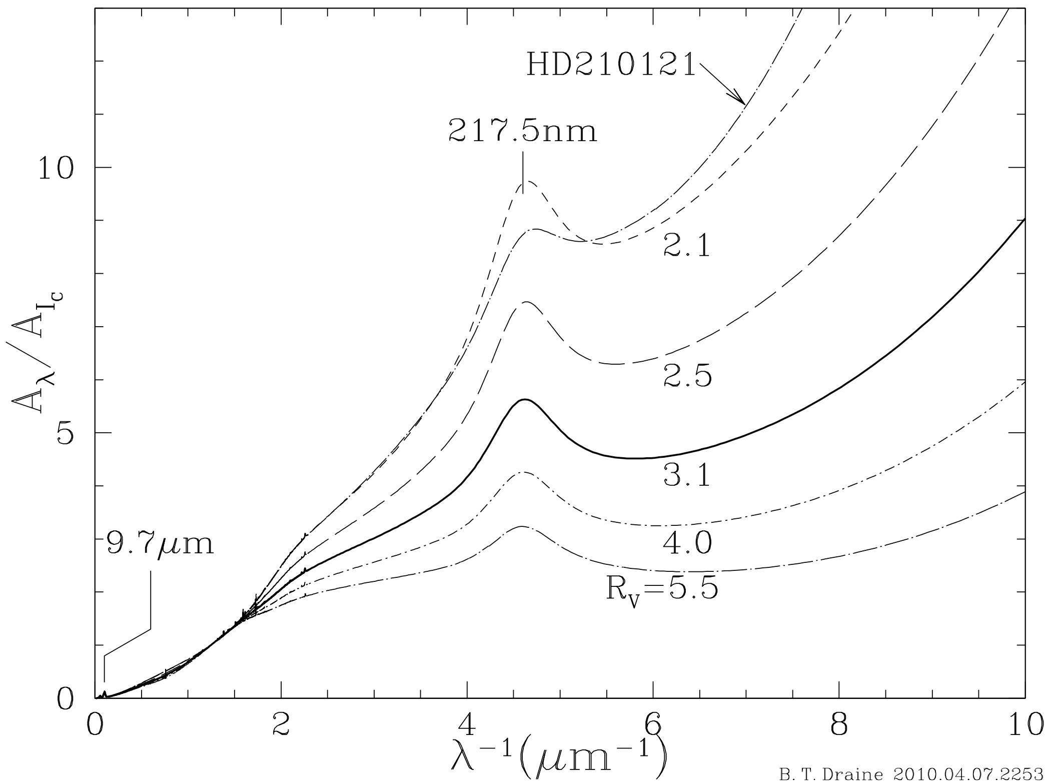

– If normalize to I_C band ($\lambda = 0.802\,\mu$m), extinction extinction is $\sim$ "universal" (?) for $\lambda \gtrsim 0.8\,\mu$m

– Significant sightline-to-sightline variation seen in visible and especially UV ($\lambda \lesssim 0.5\,\mu$m)

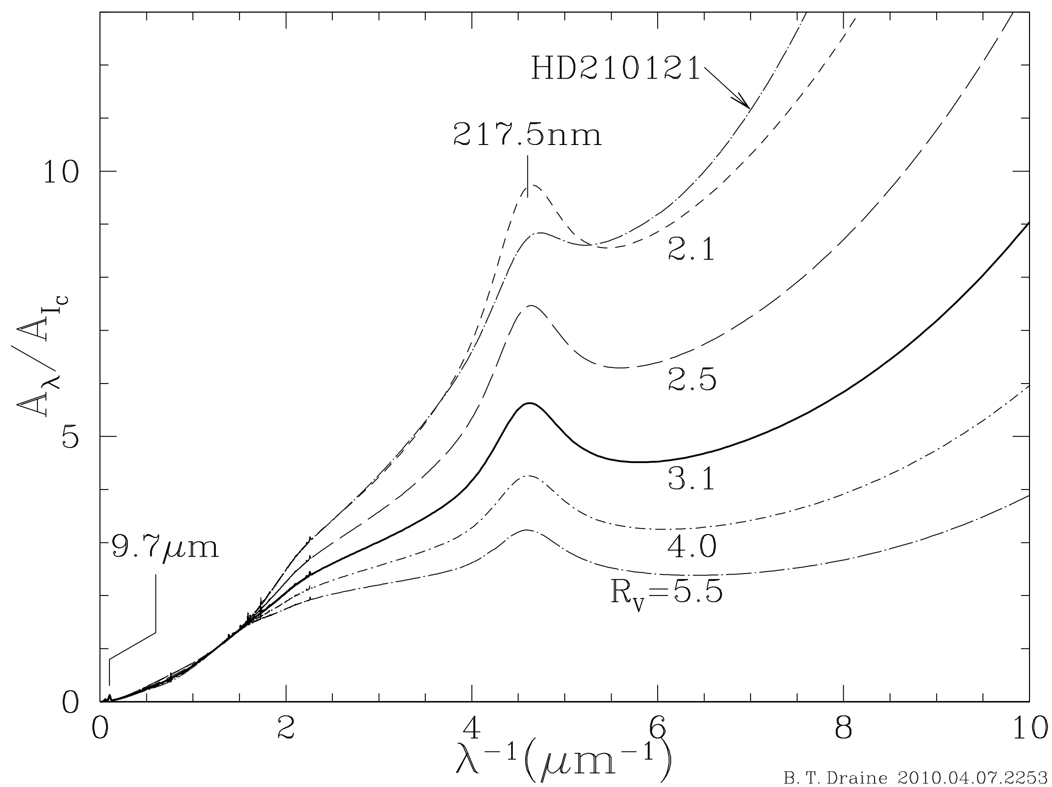

- Curves can be characterized by $R_V \equiv A_V/(A_B - A_V)$ as the parameter. On diffuse sightlines in Milky Way, R_V varies from ~ 2 to $\gtrsim 5$.
- Cardelli et al. (1989) proposed a fitting function with 7 adjustable parameters:

$$\frac{A_\lambda}{A_{\lambda,\rm ref}} = f_7(\lambda)$$

CCM found that the 7 fit parameters were all strongly-correlated with R_V. Thus the 7-parameter fit can be treated as a one-parameter family of curves, with R_V as the parameter:

$$\frac{A_\lambda}{A_{\lambda,\rm ref}} \approx f_1(\lambda; R_V)$$

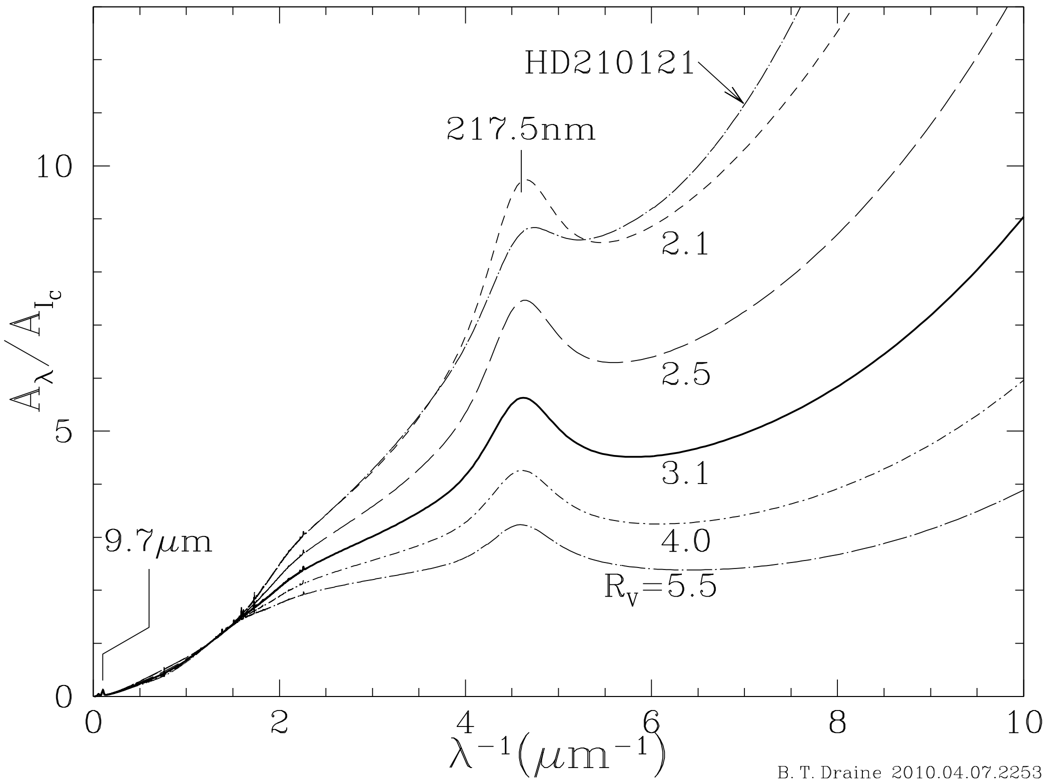

- General rise in extinction for $1 \lesssim \lambda^{-1} \lesssim 10\,\mu m^{-1}$ requires that $a \lesssim 0.1\,\mu m$ [otherwise dust would have $2\pi a/\lambda \gtrsim 1$, with extinction ∼independent of λ].
- Strong rise down to $\lambda \approx 0.1\,\mu m$ requires large abundance of grains with $2\pi a/\lambda = 2\pi a/(0.1\,\mu m) \lesssim 1$, or $a \lesssim 0.1\,\mu m/2\pi \approx 0.015\,\mu m$.
- **Conclusion:** must have a very broad size distribution, extending over at least a factor $\gtrsim 10$ in radius, or $\gtrsim 10^3$ in mass.

2. Polarization of Starlight

- Polarization of starlight discovered serendipitously (Hall 1949; Hiltner 1949)

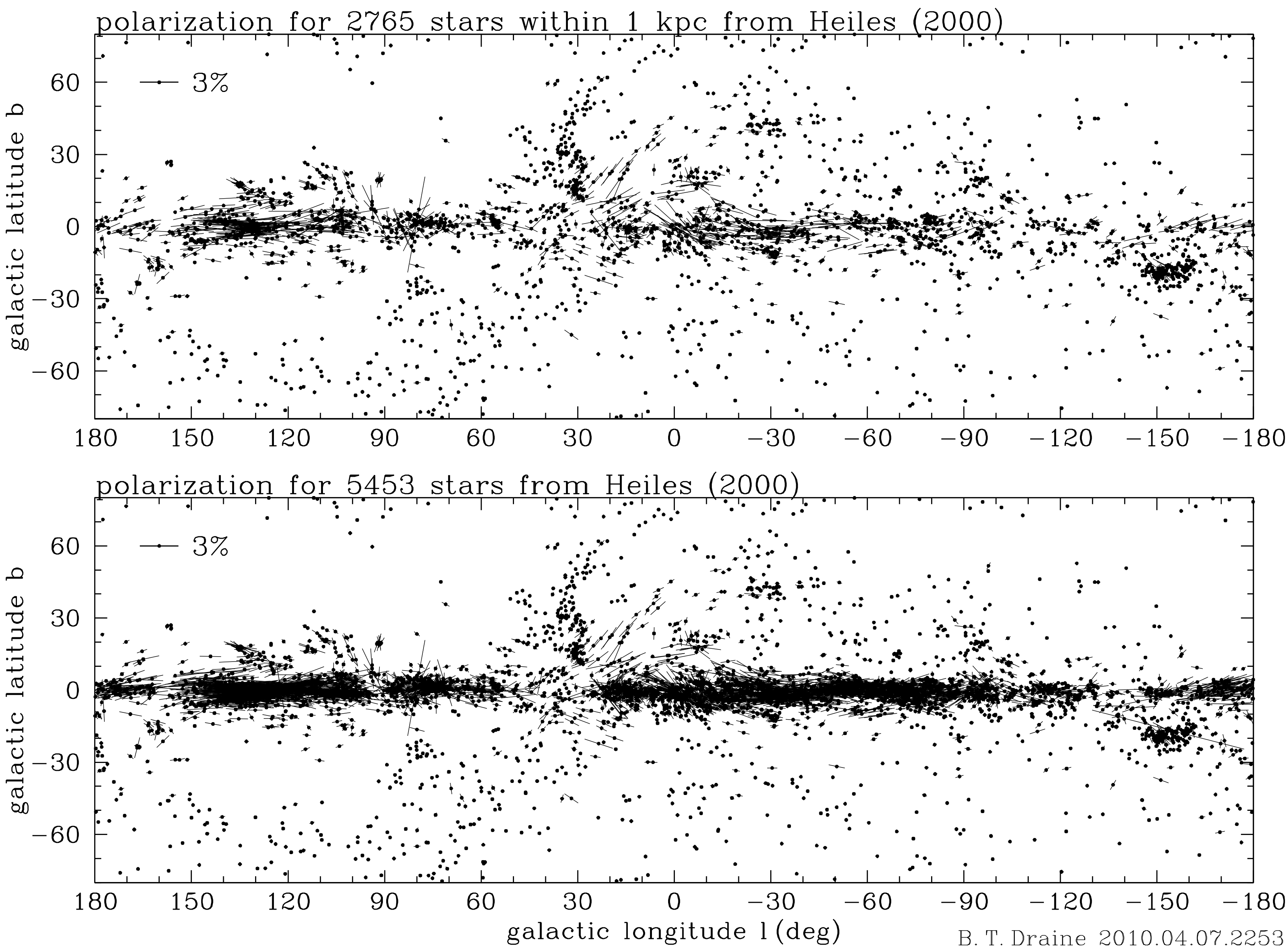

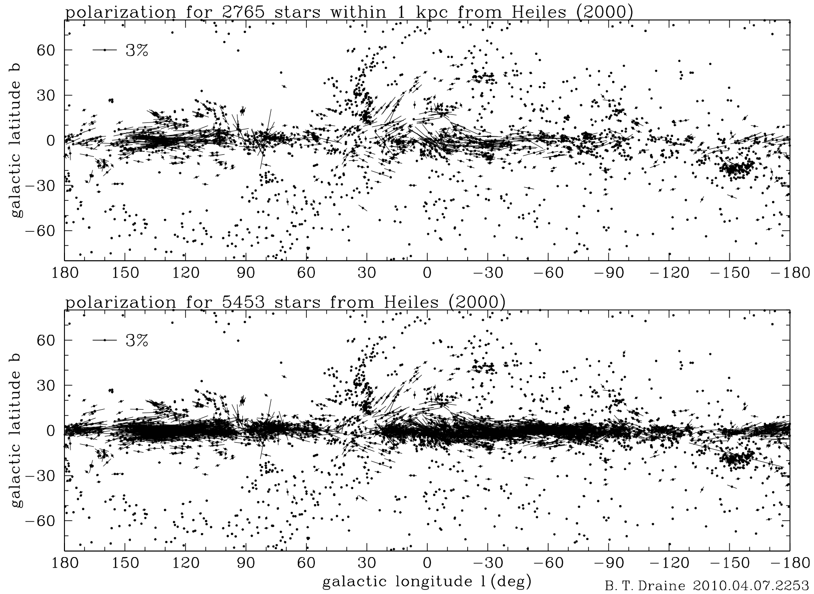

- Polarization vs. λ is *continuous* and
  Polarization is *spatially coherent*:
  - Must be produced by *interstellar dust*
  - Some of the dust grains must be *nonspherical* and *aligned*
  - Coherence: Alignment direction must be determined by interstellar $\vec{\mathbf{B}}_0$
- Polarization is *approximately* described by the "Serkowski law" (Serkowski 1973):

$$p(\lambda) = p_{\rm max} \exp\left[-K\left(\ln(\lambda/\lambda_{\rm max})\right)^2\right]$$

with $\lambda_{\rm max} \approx 0.55\,\mu{\rm m}$ and $K \approx 1.15$

$$0 \leq p_{\rm max} \lesssim \left[\frac{0.09}{E(B-V)}\right] p_{\rm max} \lesssim 0.03 A_V$$

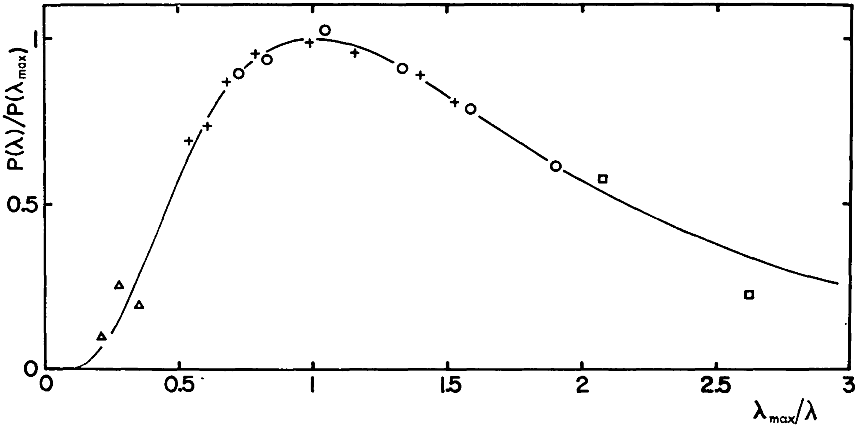

Fig. 5. Normalized wavelength dependence of interstellar polarization averaged for 6 stars in Perseus-Cepheus (crosses) for which $\lambda_{max} \cong 0.52\ \mu$ and for 5 stars in Scorpius (open circles) for which $\lambda_{max} \cong 0.70\ \mu$. Ultraviolet balloon observations for ζ Ophiuchi at $\lambda = 0.225\ \mu$ and $0.286\ \mu$ by Gehrels (1973; squares) and the infrared observations of HD 183143 at $\lambda = 1.6\ \mu$ and VI Cyg *12 at $\lambda = 1.6\ \mu$ and $\lambda = 2.2\ \mu$ by Dyck (1973; triangles) are also plotted. The solid line is calculated from Equation (1).

- Implications of Wavelength-dependence of Polarization
  - Grain optics: grains producing polarization near $\sim 0.55\,\mu\mathrm{m}$ have $2\pi a/\lambda \approx 1 \rightarrow a \approx 0.1\,\mu\mathrm{m}$.
  - $p(\lambda)/\tau_\lambda$ is very small in the UV: small grains responsible for rise in UV extinction are either *spherical* (unlikely) or *randomly-oriented.*
  - Mechanism producing alignment of interstellar grains in the diffuse ISM is size-sensitive:
    - ∗ manages to align grains with $a \gtrsim 0.1\,\mu\mathrm{m}$,
    - ∗ does *not* align grains with $a \lesssim 0.05\,\mu\mathrm{m}$.

3. Scattering of Starlight

Two Reflection Nebulae: Pleiades (M44) NGC 7023

- Dust grains produce substantial scattering at visual wavelenghts:
  - must have $2\pi a/0.55\,\mu\text{m} \gtrsim 1$, or $a \gtrsim 0.1\,\mu\text{m}$.

Also seen in UV and MIR

- Can determine scattering properties of dust (albedo and scattering phase function) by studying individual reflection nebulae (but this is not easy – requires assumptions about nebular geometry)
- Can also determine scattering properties of dust by studying the general interstellar background of scattered light – the *Diffuse Galactic Light* (but this is not easy – it it is faint)
- Usually limited to trying to estimate *albedo*≡ scattering/(scattering+absorption) and $\langle\cos\theta\rangle$, where θ = scattering angle
  Isotropic scattering or Rayleigh scattering would have $\langle\cos\theta\rangle = 0$

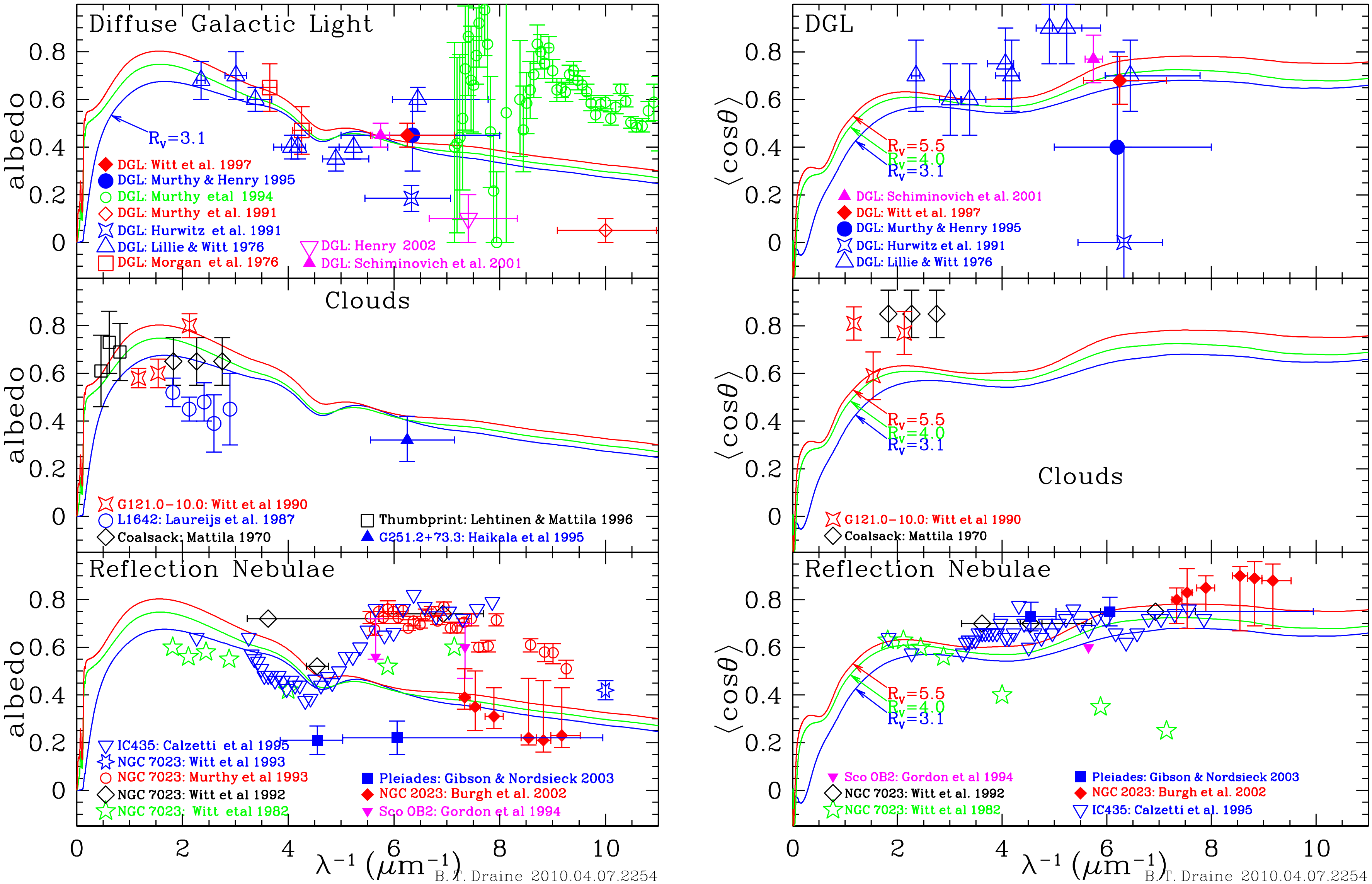

Solid curves: dust models (Weingartner & Draine 2001).

Scatter among different observational results is indication of difficulty and uncertainty

Albedo ≈ 0.5 from visible to UV

Grains are forward-scattering, $\langle\cos\theta\rangle \approx 0.6$

Observational results are $\sim$ consistent with dust models

8. Far-Infrared Emission

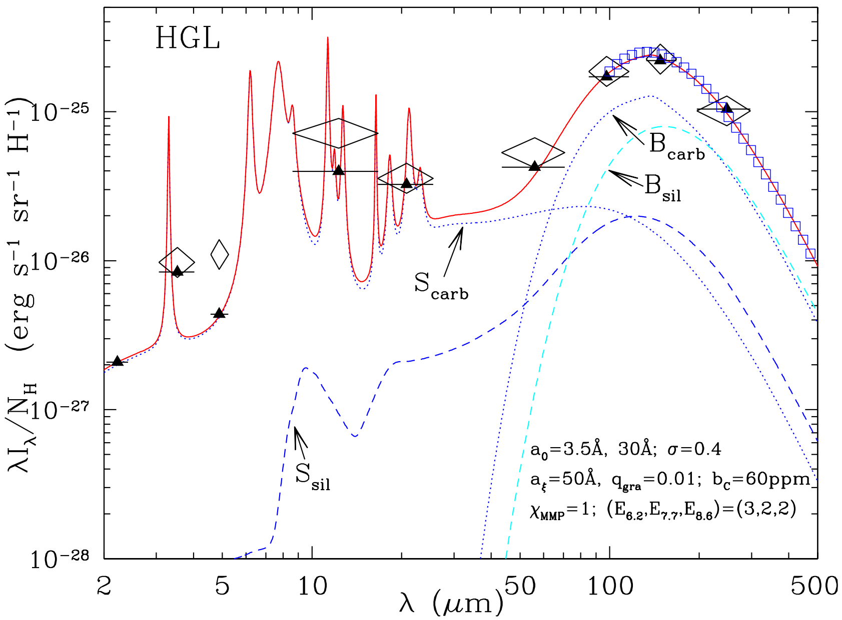

Diffuse emission at high galactic latitudes (Li & Draine 2001).

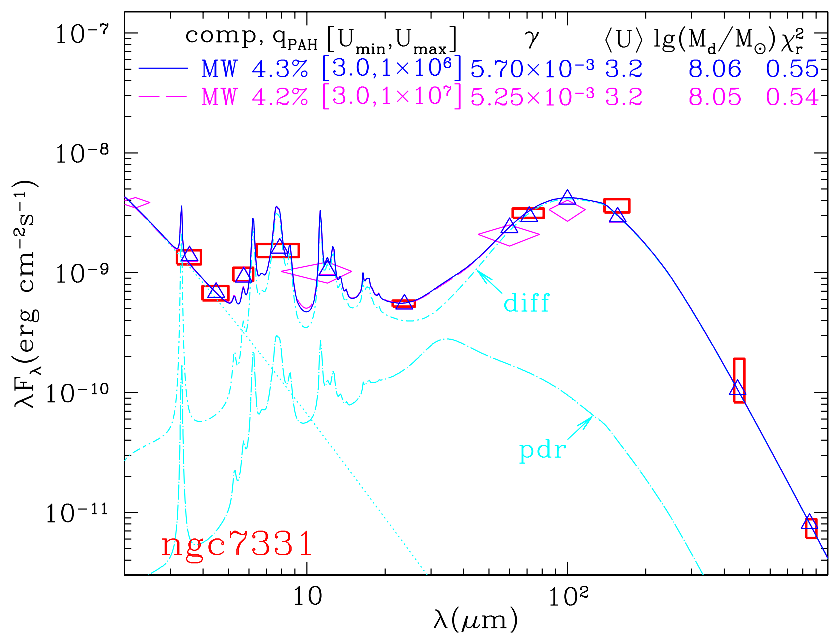

Global SED for NGC 7331 (Draine et al. 2007)

- Local emission from dust at high galactic latitudes measured by IRAS and COBE.
  - This is dust heated by starlight with spectrum and intensity similar to diffuse starlight at location of Sun.
  - Most of power radiated near $\sim$140 μm $T_d \approx (1/6)hc/\lambda_{\max}k \approx 17\,\mathrm{K}$
  - Substantial amount of power at $\lambda \lesssim 25\,\mu$m – requires dust that is much hotter than 17K
- Global emission from normal star-forming galaxies measured by is quite similar to local emission, suggesting that most IR emission from normal star-forming galaxies originates in the diffuse ISM, with most of the dust mass at $T \approx 20\,\mathrm{K}$.

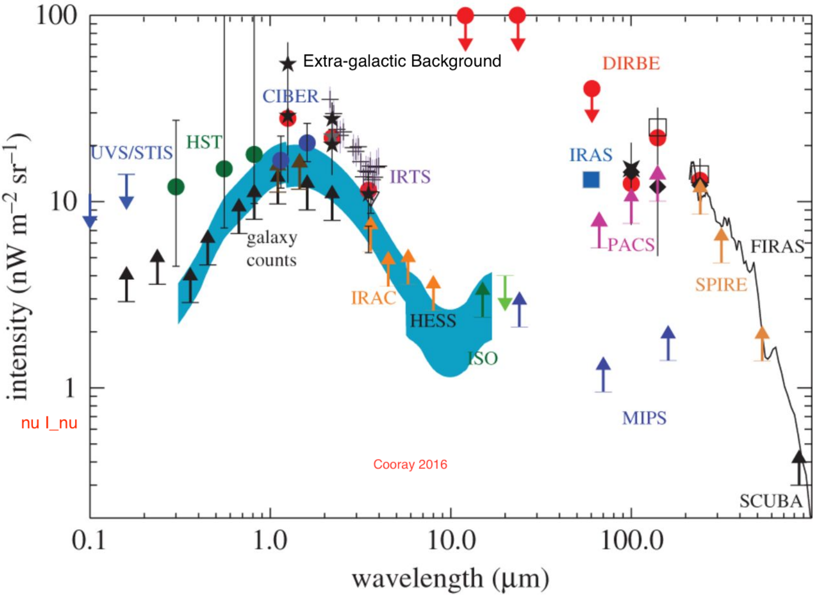

100
10
1
intensity (nW m^{-2} sr^{-1})
nu I_nu
0.1
1.0
10.0
100.0
wavelength (μm)
Extra-galactic Background
DIRBE
CIBER
UVS/STIS
HST
IRTS
IRAS
galaxy
counts
PACS
FIRAS
IRAC
HESS
SPIRE
ISO
MIPS
Cooray 2016
SCUBA

9. X-Ray Scattering by Dust

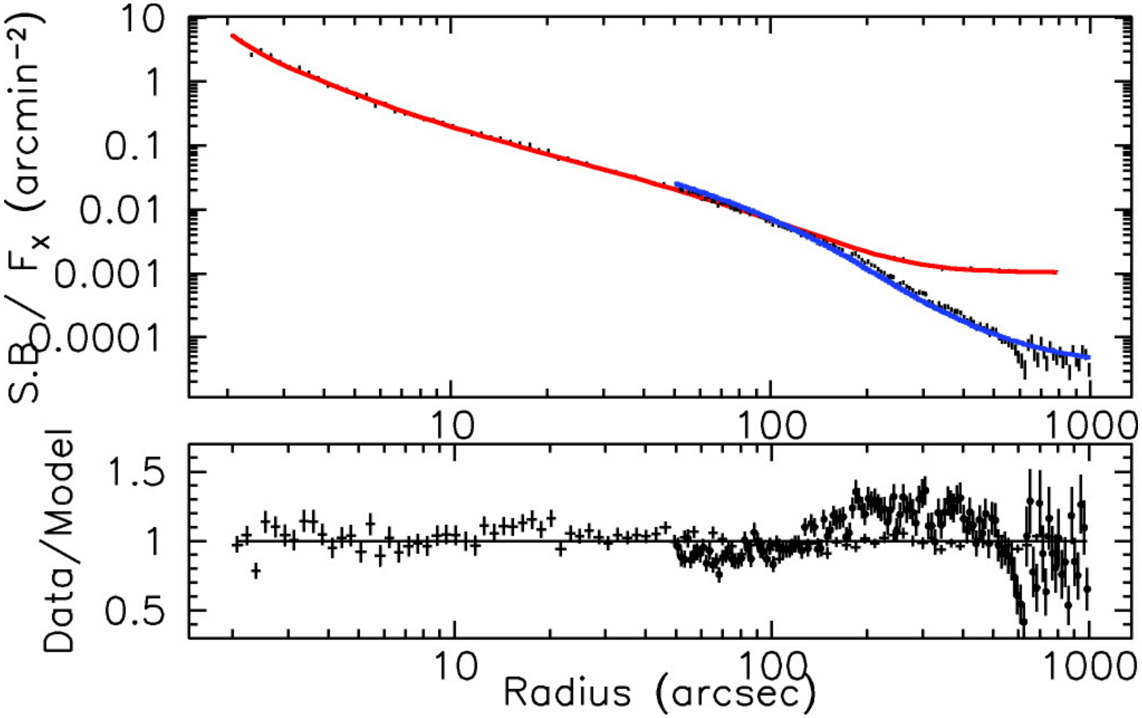

1.5-6 keV X-ray halo around GX 13+1 observed by Chandra. Model fits for HRC-1 in red, ACIS-I in blue (Smith 2008). Model = WD01 dust uniformly-distributed along LOS.

- Characteristic scattering angle

$$\theta \approx \frac{\lambda}{\pi a} = 800'' \left(\frac{keV}{h\nu} \frac{0.1\,\mu\mathrm{m}}{a} \right)$$

- Comparison with model requires assumptions about location of dust on path between source and observer (to relate observed *halo angle* to *scattering angle*).

X-Ray Halo Around GRB 050724

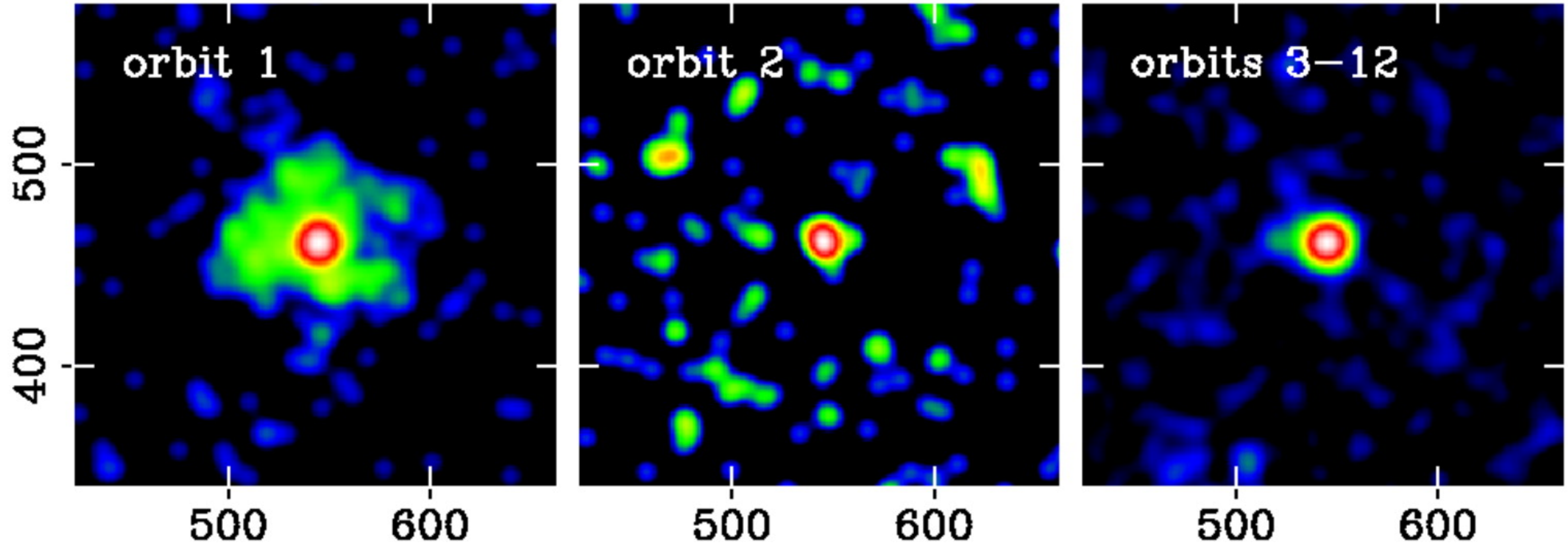

0.2–5keV X-ray images of GRB 050724 1300 ± 950s, 7000 ± 1000s, and later. From Vaughan et al. (2006).

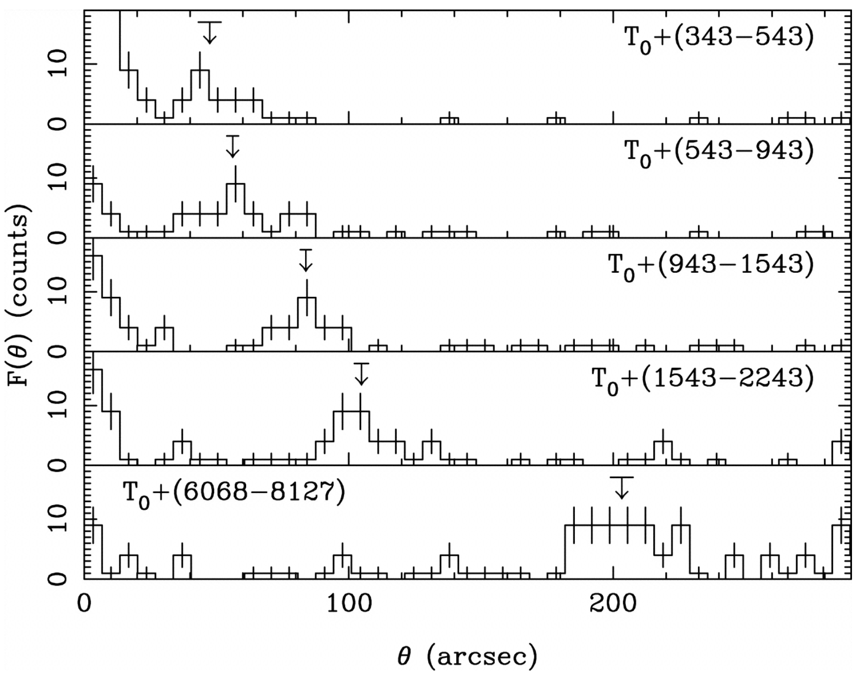

$$\Delta t = \frac{1}{2}\frac{D\theta^2}{c}$$

Dust in a sheet at distance $D \approx 139 \pm 9\,\mathrm{pc}$, $\Delta D < 22\,\mathrm{pc}$

N.B. This method could in principle be used to determine distance to M31 to absolute accuracy **$\pm 1\%$** using background AGN (Draine & Bond 2004) (all we need is $\sim$5 Ms of time on Chandra...)

10. Microwave Emission by Dust

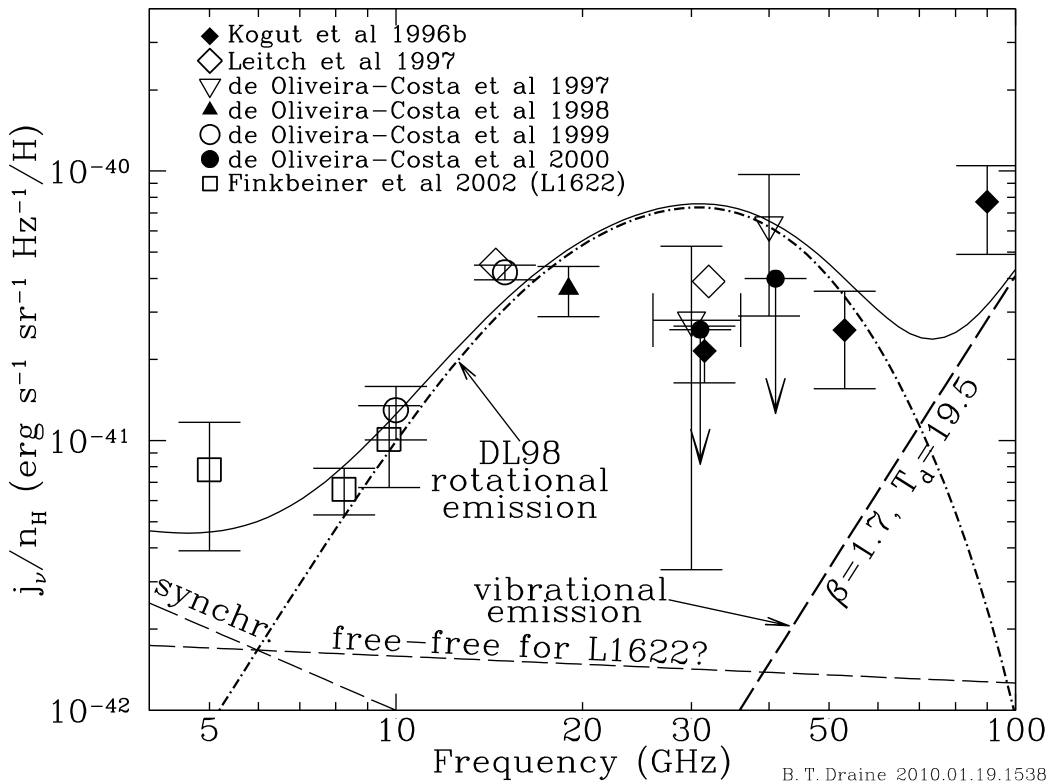

Interstellar emissivity per H nucleon

- synchrotron emission: $j_\nu \propto \nu^{-1.0}$ between 0.4 and 23 GHz
- free-free emission: $j_\nu \propto \nu^{-0.1}$
- observed *rise* in emission from 5–30 GHz cannot be explained by synchrotron or free-free: must be attributed to dust

- CMB experiments discovered microwave emission correlated with 100 μm emission from interstellar dust (Kogut et al. 1996).
- observed intensity much higher than expected from extrapolation of "normal" dust emission ("vibrational emission") to microwave frequencies
- observed intensity may be **rotational** emission from the PAH population – **"spinning dust"** (Draine & Lazarian 1998).
- Microwave emission provides another constraint on interstellar dust models.
- Observed emission places an *upper limit* on fraction of interstellar Fe that can be in metallic inclusions, as thermal fluctuations in their magnetization would generate magnetic dipole radiation at microwave frequencies.

6. Abundance Constraints

Have seen above that $M_d/M_{\rm H} \gtrsim 0.0083$. What do we expect this number to be? Measure abundances in gas and compare to solar (which we assume to be similar to *total* abundance in ISM today).

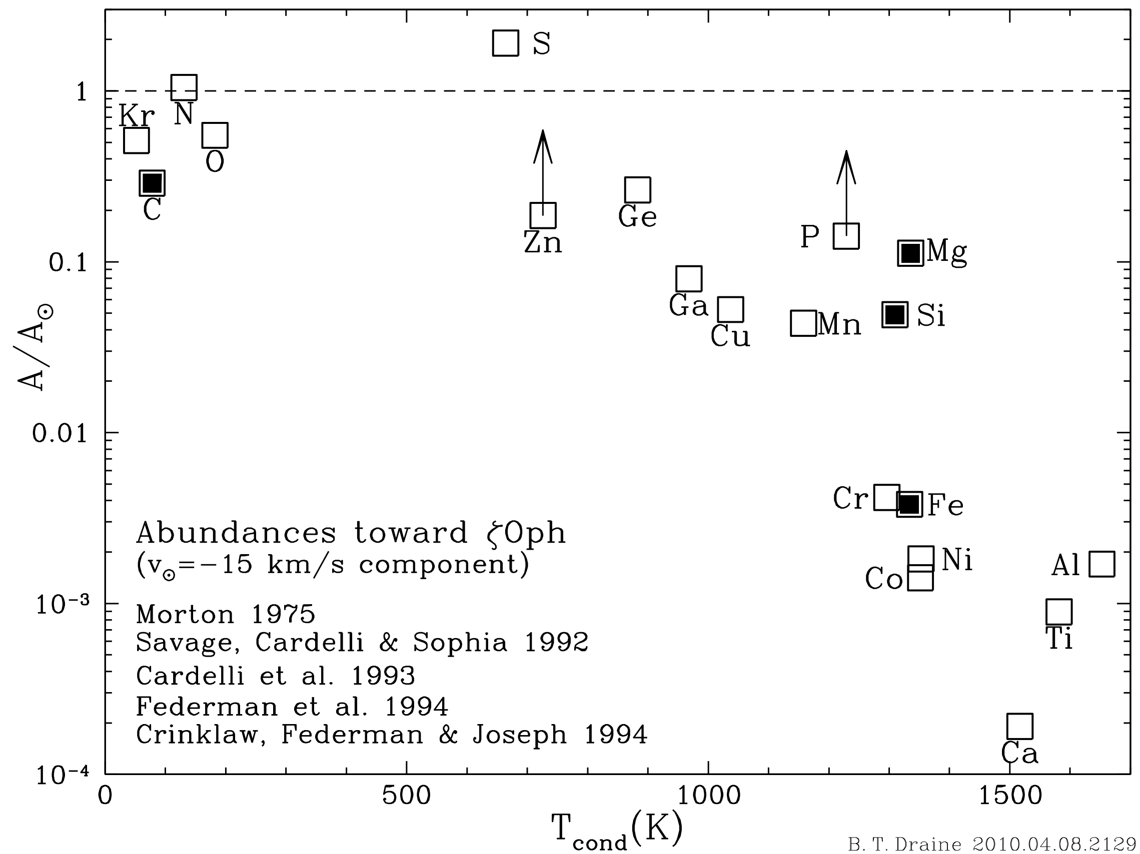

Sightline to ζOph – best-studied sightline in ISM.

- Some elements (e.g., N) are *undepleted* – abundance in gas ≈ solar.
- Some elements (e.g., Si, Fe) are very strongly depleted: $> 90\%$ is missing from gas.
- C appears to be moderately depleted: $\sim$70% of C is missing from gas.
- Missing C, Mg, Si, Al, Ca, Fe, Ni + $\sim$29% of O: $M_d/M_{\rm H} = 0.0091$

- Purcell lower limit on 0.0083 is similar to the value 0.0091 inferred from depletion studies.
- $\int C_{\rm ext} d\lambda$ must be dominated by $0.1 < \lambda < 30\,\mu{\rm m}$ range – the contribution to the integral from $\lambda > 30\,\mu{\rm m}$ must be small.
- *Very large ($\gtrsim 10\,\mu{\rm m}$) grains cannot contribute much mass.*

7.4 Diffuse Interstellar Bands (DIBs)

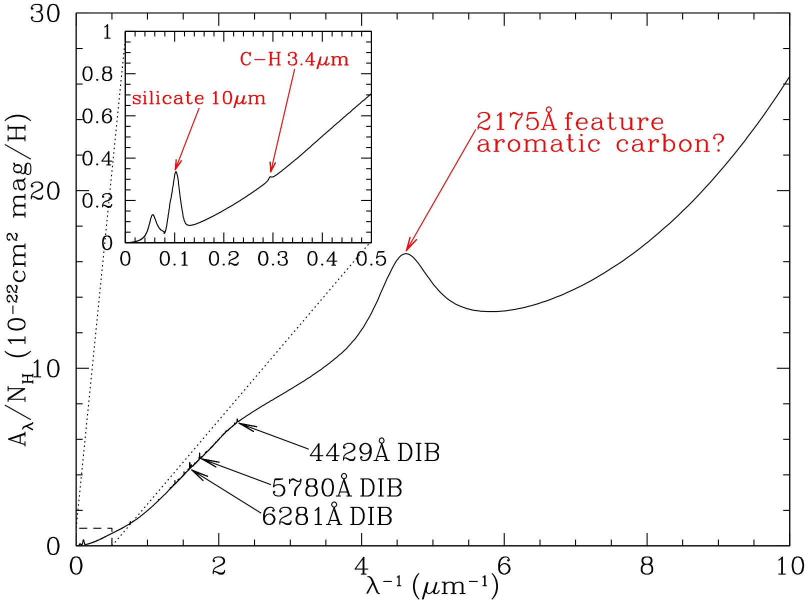

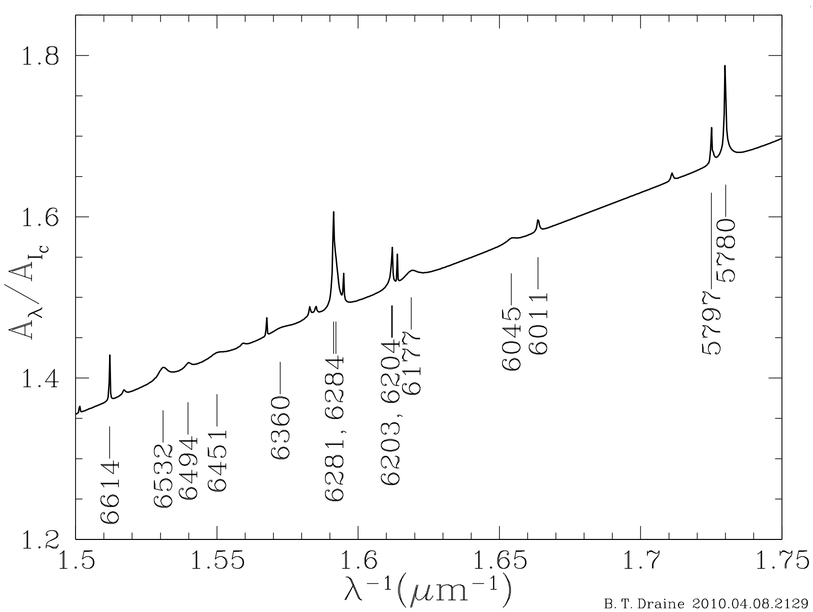

- weak but well-defined spectral features, too broad ($\Delta\lambda \sim 1$ Å) to be due to atoms, ions, or small molecules.
- First observed by Heger (1922). Recent surveys have tabulated **MANY:** **>400** between 3900 and 8100Å (Hobbs et al. 2009)
- **NONE** have been identified!
- Indications of structure (Kerr et al. 1998) consistent with molecular rotation...

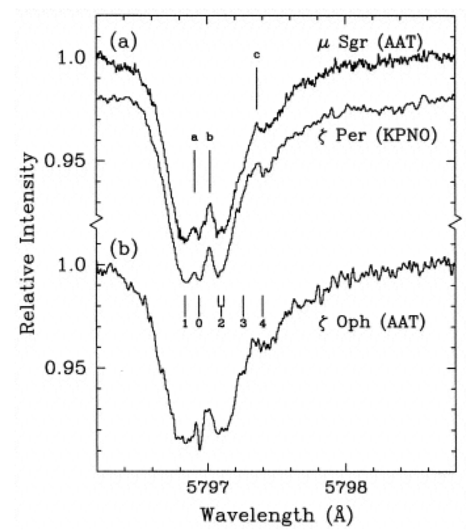

- Hypothesis: DIBs = electronic transitions in PAHs.

7.2 The Silicate Features

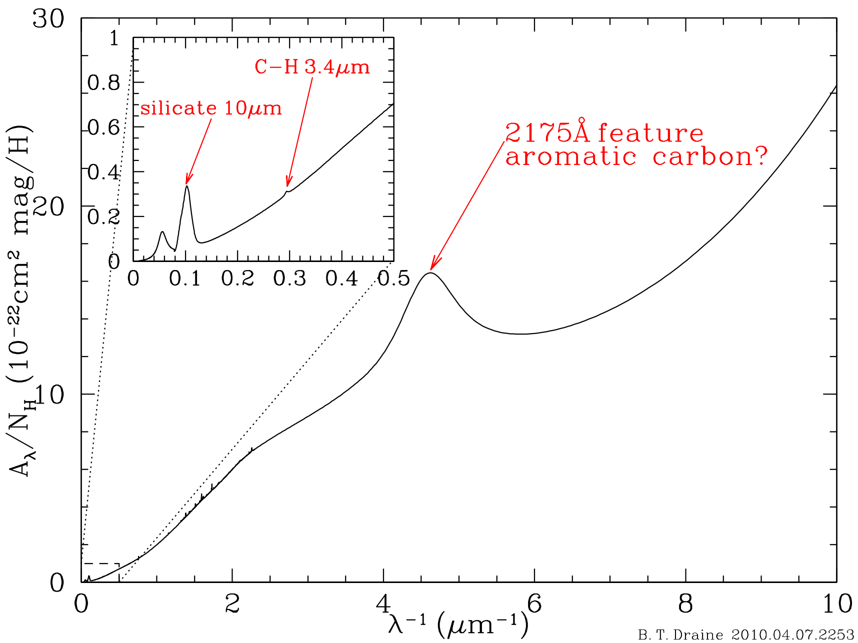

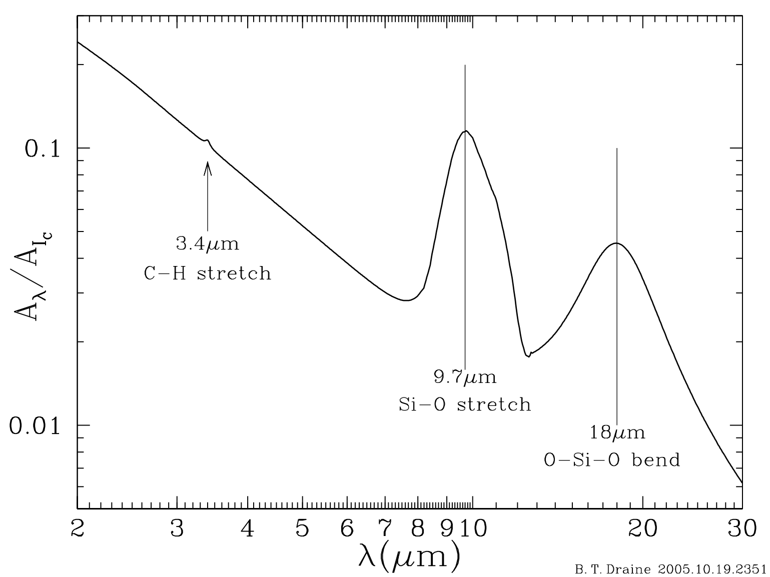

- Broad feature at $\sim$9.7 μm feature observed in absorption on sightlines with sufficient $N_{\rm H}$
- Profile consistent with Si-O stretching mode in **amorphous silicate**
- Also a weaker feature at $18\,\mu$m consistent with O-Si-O bending mode in amorphous silicates.
- Similar features seen in **emission** in winds from cool O-rich stars.
- Identification as amorphous silicate is secure
- Nearby ISM has $A_V/\Delta\tau_{9.7} \approx 18.5 \pm 2$
- Sightlines to sources near the GC have $A_V/\Delta\tau_{9.7} \approx 9 \pm 1$
- Strength of silicate profile: requires that majority of Mg, Si, and perhaps Fe be in amorphous silicates (possible composition $MgFeSiO_4$)
- Absence of sharp structure in profile: no more than **2%** of interstellar silicates are crystalline.
- Polarization in silicate feature is observed: silicate grains can be aligned in ISM

7.3 The 3.4 μm Feature

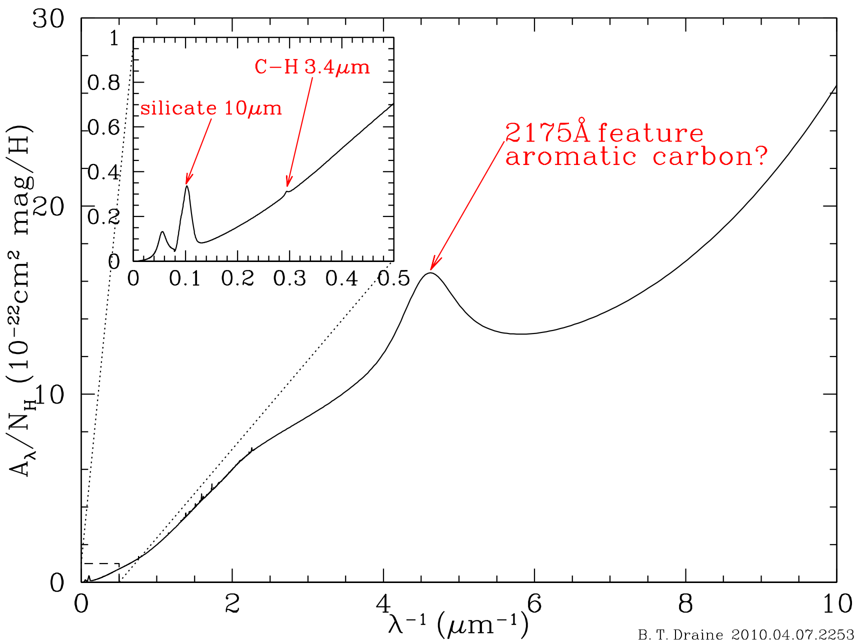

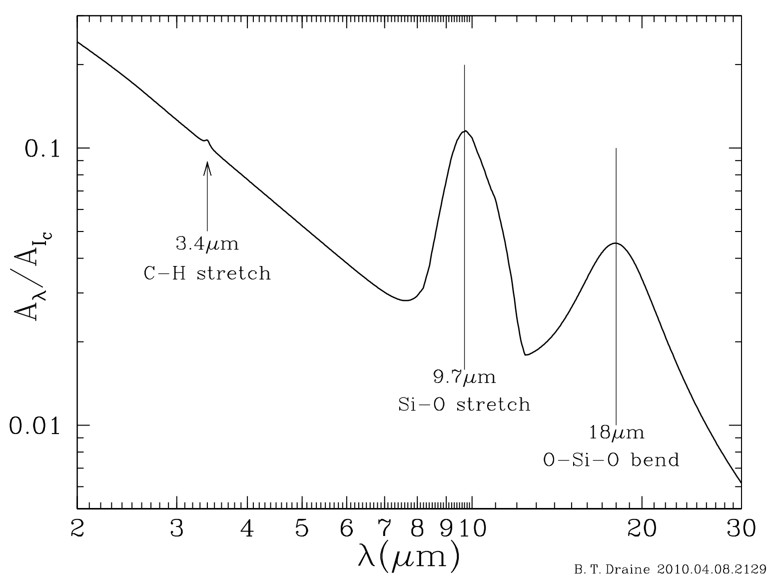

- Weak feature at $\sim$3.4 μm feature observed in absorption on sightlines with sufficient $N_{\rm H}$
- Identified as C-H stretch in hydrocarbons
- Type (and amount) of hydrocarbon is **controversial**
  - Pendleton & Allamandola (2002): $\sim$85% aromatic, $\sim$15% aliphatic
  - Dartois et al. (2004): $< 15\%$ aromatic
- $\Delta\tau_{3.4\,\mu{\rm m}}/A_V$ depends on environment: higher in HI clouds, lower in dark H_2 clouds (Shenoy et al. 2003).
  Mennella et al. (2003) suggest
  - Destruction of C-H bonds by CR in dark clouds?
  - regeneration of C-H by exposure to H in HI clouds?

7. Composition of Interstellar Dust: Observed Spectral Features

7.1 The 2175Å Feature

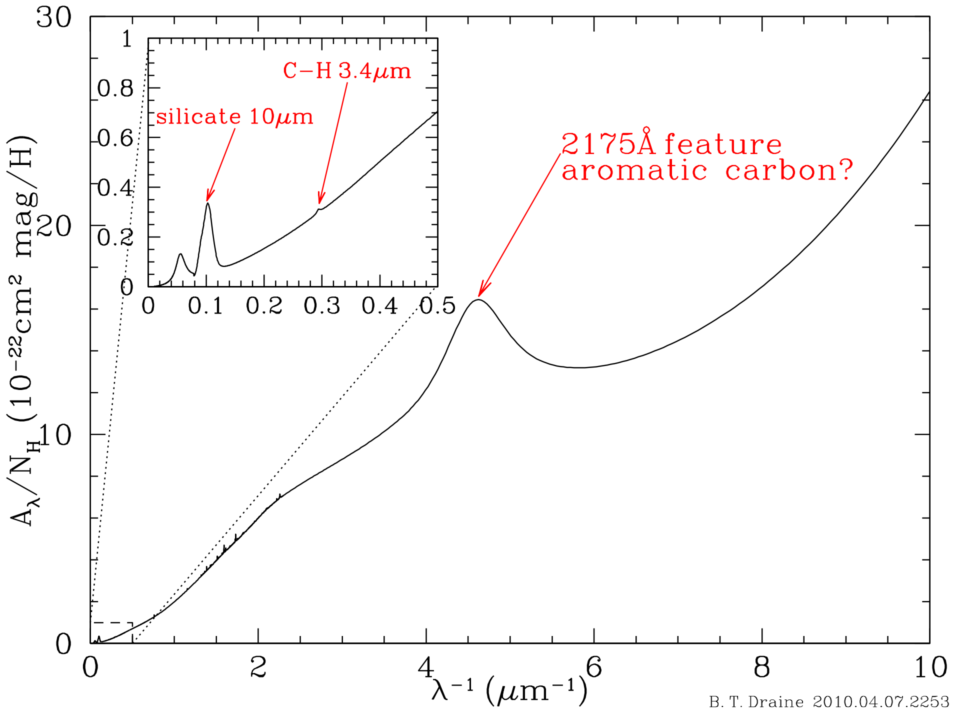

- Very strong: grain component must be abundant. Must come from compound of some subset of $\{\mathrm{C}, \mathrm{O}, \mathrm{Mg}, \mathrm{Si}, \mathrm{Fe}\}$ – other elements not abundant enough.
- In good agreement with calculations of absorption by randomly-oriented spheres of graphite: absorption comes from $\pi \rightarrow \pi^*$ excitations of π electrons in the graphite basal plane.
- Large PAH molecules have C in sheets of hexagons (sp^2-bonding) just as in graphite. Also have strong absorption in neighborhood of 2200Å
- Little or no polarization in 2200Å feature
- Current estimates of PAH abundance – (C in PAHs)/H ≈ 55ppm – suggest that **2200Å feature is probably due to C in PAHs**.
- Other carriers have been proposed (e.g., MgO).

7.5 Ice Features in Dark Clouds

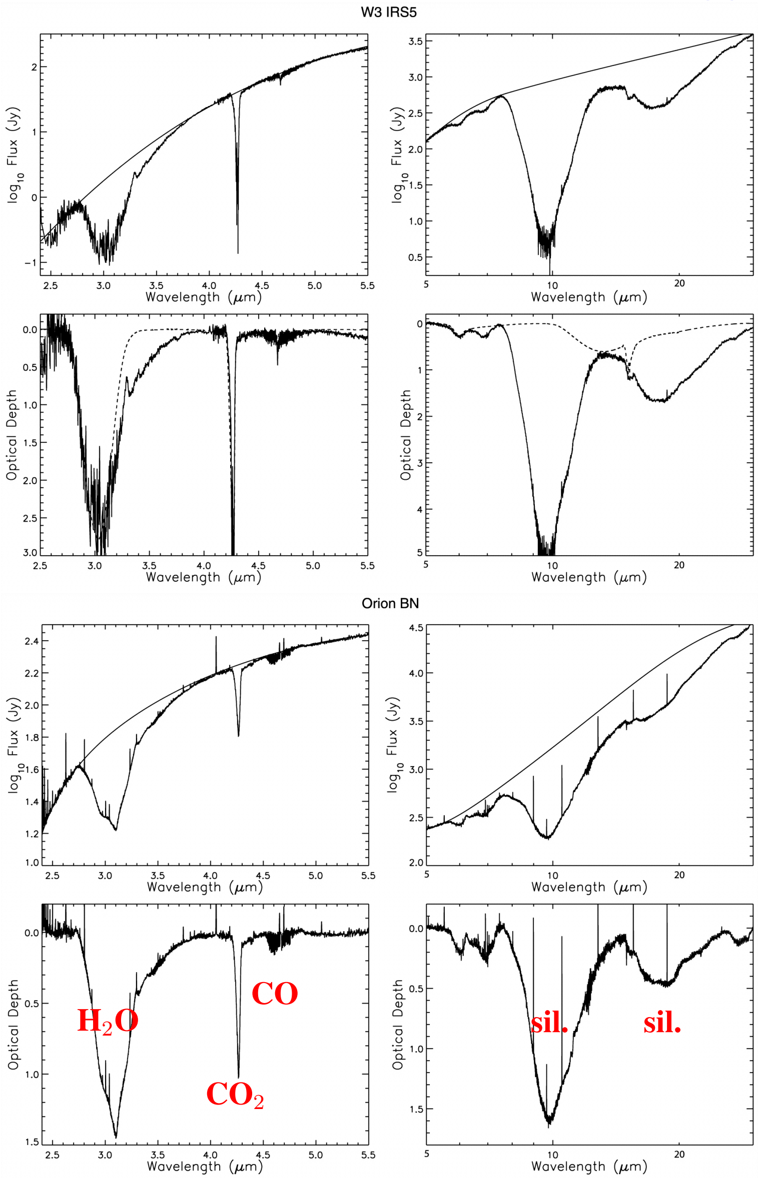

ISO spectra of W3 IRS5 and Orion BN (Gibb et al. 2004).

- **Predominantly H_2O** ice but also CO, CO_2, NH_3, CH_3OH, ...

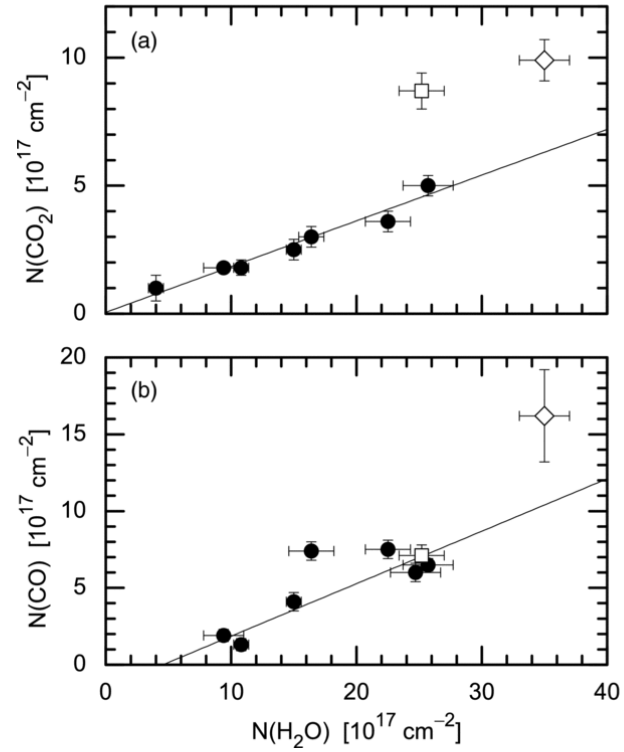

(From Whittet et al. 2009)

- Ice can increase total grain volume by factor of up to ~ 2.
- **ONLY** in **DARK** clouds with $A_V \gtrsim 3.3\,\text{mag}$:

$$\Delta\tau_{3.1} \approx 0 \qquad \text{for } A_V < 3.3\,\text{mag}$$
$$\Delta\tau_{3.1} \approx 0.093[A_V - 3.3\,\text{mag}] \qquad \text{for } A_V > 3.3\,\text{mag}$$

- **Photodesorption by UV removes H_2O from dust in diffuse clouds.**

7.6 Polycyclic Aromatic Hydrocarbons in Emission

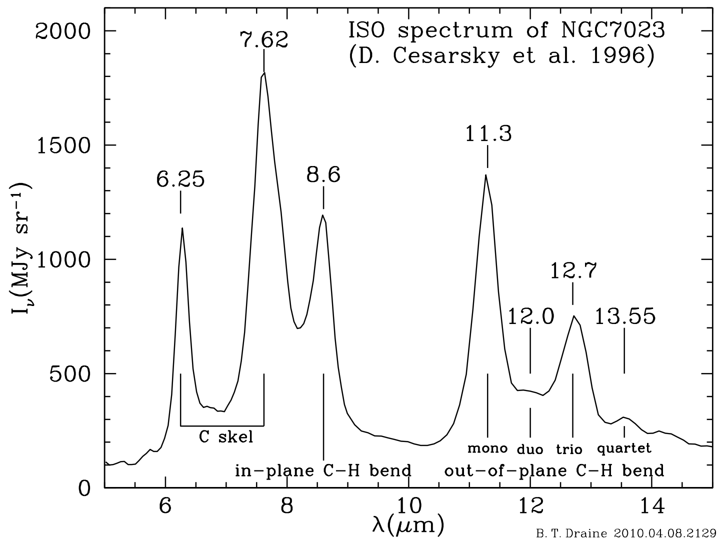

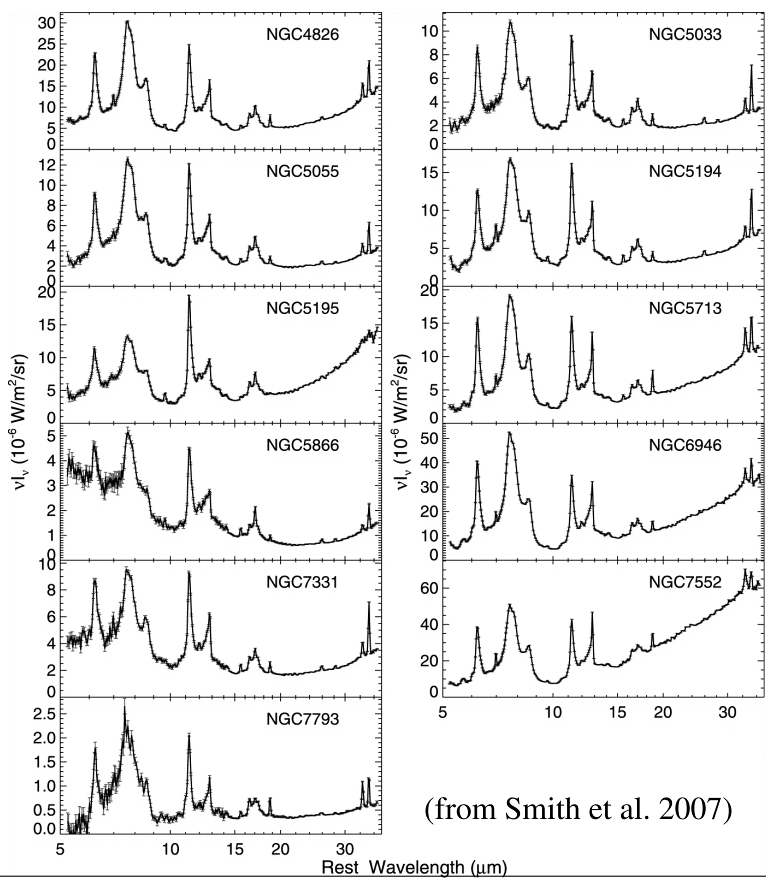

(from Smith et al. 2007)

- IR emission features at 3.3, 6.2, 7.6, 8.6, 11.3, 12.7 correspond to vibrational modes of **polycyclic aromatic hydrocarbons (PAHs)**.
- For normal star-forming galaxies, integrated emission in PAH features can be up to 20% of total IR emission.
- This requires that PAHs be abundant enough to account for up to 20% of the starlight absorption.
- Required PAH abundance: **at least $\sim$5% of the total grain mass contributed by PAHs in the MW**.

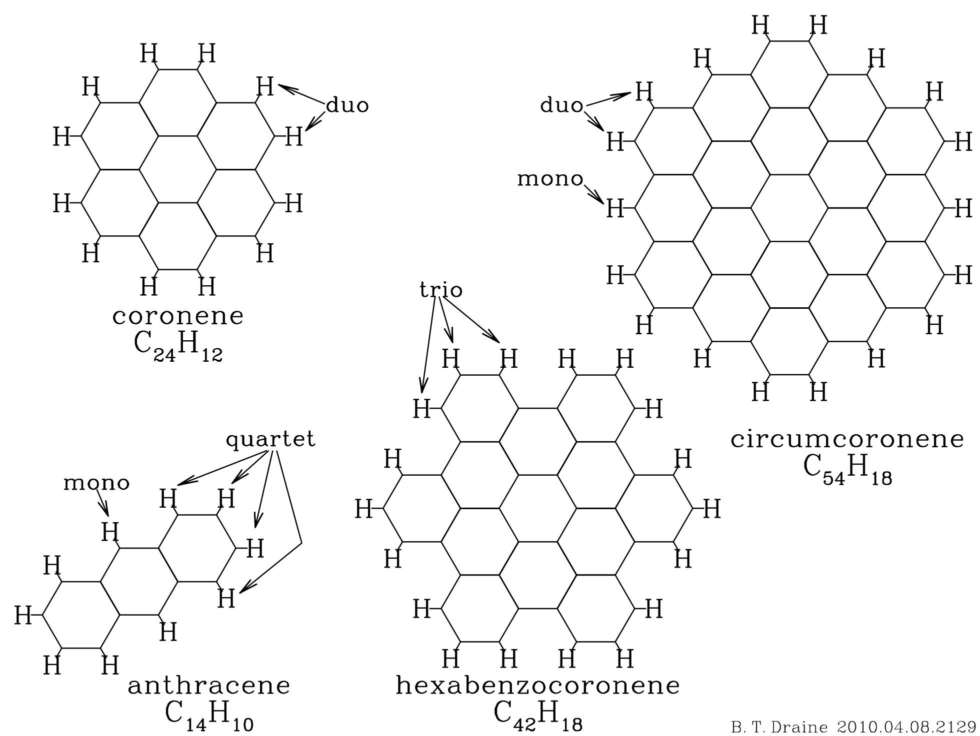

11. Dust in Meteorites

Types and properties of major presolar materials⋆ identified in meteorites and IDPs. See Huss & Draine (2007) and references therein.

Material	Source	Grain Size (μm)	Abundance (ppm)†
Amorphous silicates	circumstellar	0.2-0.5	20-3600
Forsterite (Mg_2SiO_4) } Enstatite ($MgSiO_3$)	circumstellar	0.2-0.5	10-1800
Diamond		∼0.002	∼1400
P3 fraction	?		
HL fraction	circumstellar		
Silicon carbide	circumstellar	0.1-20	13-14
Graphite	circumstellar	0.1-10	7-10
Spinel ($MgAl_2O_4$)	circumstellar	0.1-3	1.2
Corundum (Al_2O_3)	circumstellar	0.5-3	0.01
Hibonite ($CaAl_{12}O_{19}$)	circumstellar	1-2	0.02
TOTAL	circumstellar	0.002-20	**1450-6800**

⋆Other presolar materials include TiC, MoC, ZrC, RuC, FeC, Si_3N_4, TiO_2, and Fe-Ni metal.

†Abundance in fine-grained fraction (= matrix in primitive chondrites).

- Presolar grains are identified by isotopic anomalies – must differ from *average* isotopic ratios in protosolar nebula.
- Grains with isotopic anomalies will generally be **stardust** – grains formed in outflows from individual stars with their particular isotopic composition.
- **(0.4±0.25)%** of mass in primitive meteorite is **stardust**
- Such grains were part of ISM 4.567 Gyr ago – but they may have been a minority fraction of interstellar dust.
- Should be cautious about relating *stardust in meteorites* to the *interstellar grain population*.

4. The Volume of Interstellar Dust: The Purcell Limit

Dust models normally proceed by experimenting with different compositions and size distributions to try to reproduce the wavelength-dependent extinction and scattering.
If successful model is found, then can calculate volume and mass of grain material, but result is clearly model-dependent.
Purcell (1969) applied a very general argument to obtain a *lower bound* on the dust volume with very few assumptions.

- Analyze **dielectric function** $\epsilon_{\rm ISM}(\omega)$ of interstellar medium.
- $\epsilon_{\rm ISM}(\omega)$ describes response (polarization) of ISM due to applied stress (E)
- Attenuation of EM plane wave $\propto \epsilon_{\rm ISM,2} \equiv {\rm Im}\left[\epsilon_{\rm ISM}(\omega)\right]$.
  Attenuation includes both **absorption** *and* **scattering**.
- Kramers-Kronig relations apply to *any* linear response function – based only on assumption of *causality*: response (polarization) depends only on applied stress ($E(t)$) in the past, not in future.

$$\epsilon_1(\omega) - 1 = \frac{2}{\pi} P \int_0^\infty dx \frac{x\epsilon_2(x)}{x^2 - \omega^2}$$

- Consider *static* dielectric function $\epsilon(\omega = 0)$:

$$\epsilon_{\rm ISM,1}(0) - 1 = \frac{2}{\pi} \int_0^\infty dx \frac{\epsilon_{\rm ISM,2}(x)}{x}$$

$$\omega \times \epsilon_{\rm ISM,2}(\omega) \quad \propto \quad n_d \, C_{\rm ext}(\omega)$$

$$[\epsilon_{\rm ISM,1}(\omega = 0) - 1] \;\; \propto \;\; n_d V_d \times F(\text{shape, dielectric function of grain material})$$

$$n_d \, V_d \times F \quad \propto \quad \int_0^\infty d\omega \, \frac{n_d \, C_{\rm ext}(\omega)}{\omega^2} \quad \propto \quad \int_0^\infty d\lambda \, n_d \, C_{\rm ext}(\lambda)$$

Result:

$$\frac{n_d V_d}{n_{\rm H}} = \frac{1}{3\pi^2 F({\rm shape},\epsilon_0)} \int_0^\infty d\lambda \, \frac{n_d}{n_{\rm H}} C_{\rm ext}(\lambda)$$
$$= \frac{1}{3\pi^2 F({\rm shape},\epsilon_0)} \int_0^\infty d\lambda \, \frac{\tau_\lambda}{N_{\rm H}} \quad . \qquad (7)$$

The dimensionless function $F({\rm shape},\epsilon_0)$ [ϵ_0 = dielectric function of the grain material] is the orientationally-averaged static polarizability relative to the polarizability of an equal-volume conducting sphere.
Likely insulating materials have finite $4 \lesssim \epsilon_0 \lesssim 10$; conductors have $\epsilon_0 \to \infty$

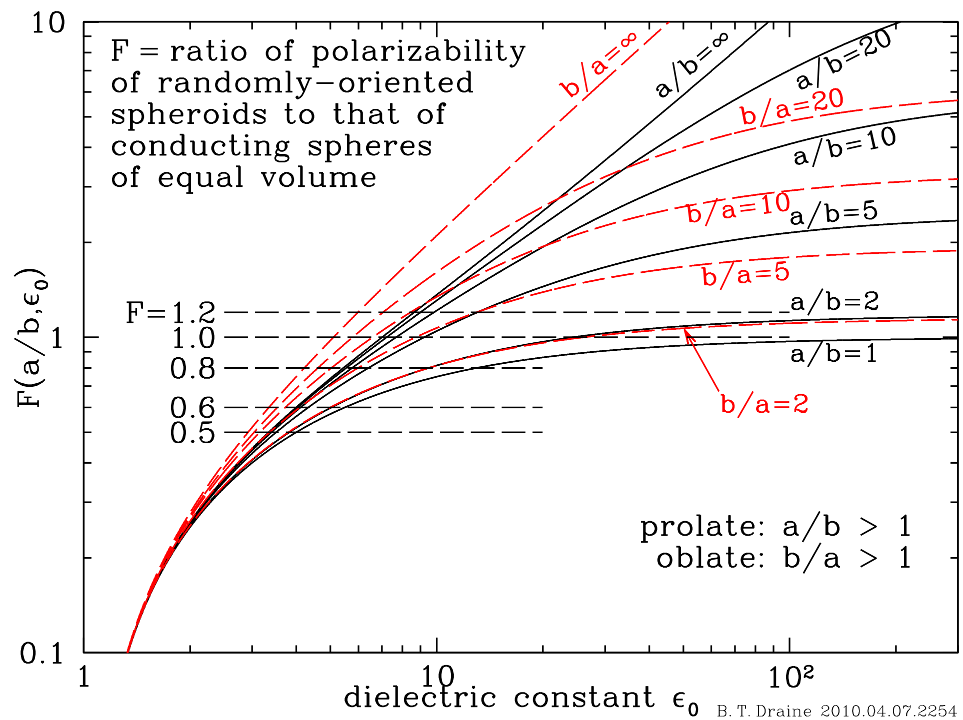

Result: $0.5 < F < 1.2$ **unless grains have extreme shapes (**$a/b > 2$ **or** $b/a > 2$ ***and*** **are conducting.**

$$\frac{n_d V_d}{n_{\rm H}} = \frac{1}{3\pi^2 F(\epsilon_0, {\rm shape})} \int_0^\infty d\lambda \frac{\tau_{\rm ext}(\lambda)}{N_{\rm H}} \quad .$$

We have measurements of $\tau_{\rm ext}(\lambda)/N_{\rm H}$ for $0.1 \lesssim \lambda \lesssim 30\,\mu{\rm m}$.

$$\int_{0.1\,\mu{\rm m}}^{30\,\mu{\rm m}} \frac{\tau_{\rm ext}}{N_{\rm H}} d\lambda \approx 1.1 \times 10^{-25}\,{\rm cm}^3/{\rm H} \quad . \tag{8}$$

Approximately half of this integral is contributed by $0.1 < \lambda < 1\,\mu{\rm m}$, and half by $1 < \lambda < 30\,\mu{\rm m}$. At other wavelengths $\tau_{\rm ext}(\lambda)/N_{\rm H}$ is not well-determined, except that we know that it must be > 0.

This gives us a lower bound on the volume of grain material per H nucleon:

$$\frac{n_d V_d}{n_{\rm H}} \gtrsim 3.7 \times 10^{-27} F^{-1} \frac{{\rm cm}^3}{\rm H}$$

If the grain material has solid density ρ_d, we have a lower bound on the *mass* of grain material relative to H mass:

$$\frac{M_d}{M_{\rm H}} \gtrsim 0.0056 \left(\frac{1.2}{F}\right) \left(\frac{\rho_d}{3\,{\rm g\,cm}^{-3}}\right)$$

where $\rho_d = 3\,{\rm g\,cm}^{-3}$ is intermediate between the density of graphite ($\rho = 2.2\,{\rm g\,cm}^{-3}$) and crystalline olivine with composition $MgFeSiO_4$ ($\rho \approx 3.8\,{\rm g\,cm}^{-3}$).

A reasonable estimate for F might be $F \approx 0.8$, in which case the Kramers-Kronig argument gives

$$\frac{M_d}{M_{\rm H}} \gtrsim 0.0083 \left(\frac{\rho_d}{3\,{\rm g\,cm}^{-3}}\right)$$

This is a *lower bound* – have neglected contributions to $\int C_{\rm ext}(\lambda) d\lambda$ from $\lambda < 0.1\,\mu{\rm m}$ and $\lambda > 30\,\mu{\rm m}$.

5. Asymptotic Behavior at Long Wavelengths

- Suppose that

$$C_{\rm ext}(\lambda) \quad \propto \quad \lambda^{-\beta} \qquad \text{for} \;\; \lambda \to \infty$$

- The Kramers-Kronig integral

$$\int_0^\infty C_{\rm ext}\, d\lambda$$

  would be divergent for $\beta \leq 1$.
  Must have $\beta > 1$ to avoid divergence.

References

Burgh, E. B., McCandliss, S. R., & Feldman, P. D. 2002, *Ap. J.*, 575, 240

Calzetti, D., Bohlin, R. C., Gordon, K. D., Witt, A. N., & Bianchi, L. 1995, *Ap. J. Lett.*, 446, L97

Cardelli, J. A., Clayton, G. C., & Mathis, J. S. 1989, *Ap. J.*, 345, 245

Cardelli, J. A., Mathis, J. S., Ebbets, D. C., & Savage, B. D. 1993, *Ap. J. Lett.*, 402, L17

Cesarsky, D., Lequeux, J., Abergel, A., Perault, M., Palazzi, E., Madden, S., & Tran, D. 1996, *Astr. Ap.*, 315, L305

Crinklaw, G., Federman, S. R., & Joseph, C. L. 1994, *Ap. J.*, 424, 748

Dartois, E., Muñoz Caro, G. M., Deboffle, D., & d'Hendecourt, L. 2004, *Astr. Ap.*, 423, L33

de Oliveira-Costa, A., Devlin, M. J., Herbig, T., Miller, A. D., Netterfield, C. B., Page, L. A., & Tegmark, M. 1998, *Ap. J. Lett.*, 509, L77

de Oliveira-Costa, A., Kogut, A., Devlin, M. J., Netterfield, C. B., Page, L. A., & Wollack, E. J. 1997, *Ap. J. Lett.*, 482, L17

de Oliveira-Costa, A., Tegmark, M., Gutierrez, C. M., Jones, A. W., Davies, R. D., Lasenby, A. N., Rebolo, R., & Watson, R. A. 1999, *Ap. J. Lett.*, 527, L9

Draine, B. T., & Bond, N. A. 2004, *Ap. J.*, 617, 987

Draine, B. T., et al. 2007, *Ap. J.*, 663, 866

Draine, B. T., & Lazarian, A. 1998, *Ap. J. Lett.*, 494, L19

Federman, S. R., Sheffer, Y., Lambert, D. L., & Gilliland, R. L. 1993, *Ap. J. Lett.*, 413, L51

Finkbeiner, D. P., Schlegel, D. J., Frank, C., & Heiles, C. 2002, *Ap. J.*, 566, 898

Gibb, E. L., Whittet, D. C. B., Boogert, A. C. A., & Tielens, A. G. G. M. 2004, *Ap. J. Suppl.*, 151, 35

Gibson, S. J., & Nordsieck, K. H. 2003, *Ap. J.*, 589, 362

Gordon, K. D., Witt, A. N., Carruthers, G. R., Christensen, S. A., & Dohne, B. C. 1994, *Ap. J.*, 432, 641

Haikala, L. K., Mattila, K., Bowyer, S., Sasseen, T. P., Lampton, M., & Knude, J. 1995, *Ap. J. Lett.*, 443, L33

Hall, J. S. 1949, Science, 109, 166

Heger, M. L. 1922, Lick Observatory Bulletin, 10, 141

Heiles, C. 2000, *A.J.*, 119, 923

Henry, R. C. 2002, *Ap. J.*, 570, 697

Hiltner, W. A. 1949, Science, 109, 165

Hobbs, L. M., et al. 2009, *Ap. J.*, 705, 32

Hurwitz, M., Bowyer, S., & Martin, C. 1991, *Ap. J.*, 372, 167

Huss, G. R., & Draine, B. T. 2007, *Highlights of Astronomy*, 14, 353

Kerr, T. H., Hibbins, R. E., Fossey, S. J., Miles, J. R., & Sarre, P. J. 1998, *Ap. J.*, 495, 941

Kogut, A., Banday, A. J., Bennett, C. L., Gorski, K. M., Hinshaw, G., Smoot, G. F., & Wright, E. I. 1996, *Ap. J. Lett.*, 464, L5

Laureijs, R. J., Mattila, K., & Schnur, G. 1987, *Astr. Ap.*, 184, 269

Lehtinen, K., & Mattila, K. 1996, *Astr. Ap.*, 309, 570

Leitch, E. M., Readhead, A. C. S., Pearson, T. J., & Myers, S. T. 1997, *Ap. J. Lett.*, 486, L23

Li, A., & Draine, B. T. 2001, *Ap. J.*, 554, 778

Lillie, C. F., & Witt, A. N. 1976, *Ap. J.*, 208, 64

Mattila, K. 1970, *Astr. Ap.*, 9, 53

Mennella, V., Baratta, G. A., Esposito, A., Ferini, G., & Pendleton, Y. J. 2003, *Ap. J.*, 587, 727

Morgan, D. H., Nandy, K., & Thompson, G. I. 1976, *M.N.R.A.S.*, 177, 531

Morton, D. C. 1975, *Ap. J.*, 197, 85

Murthy, J., Dring, A., Henry, R. C., Kruk, J. W., Blair, W. P., Kimble, R. A., & Durrance, S. T. 1993, *Ap. J. Lett.*, 408, L97

Murthy, J., & Henry, R. C. 1995, *Ap. J.*, 448, 848

Murthy, J., Henry, R. C., & Holberg, J. B. 1994, *Ap. J.*, 428, 233

Pendleton, Y. J., & Allamandola, L. J. 2002, *Ap. J. Suppl.*, 138, 75

Purcell, E. M. 1969, *Ap. J.*, 158, 433

Savage, B. D., Cardelli, J. A., & Sofia, U. J. 1992, *Ap. J.*, 401, 706

Schiminovich, D., Friedman, P. G., Martin, C., & Morrissey, P. F. 2001, *Ap. J. Lett.*, 563, L161

Serkowski, K. 1973, in IAU Symp. 52: Interstellar Dust and Related Topics, ed. J. M. Greenberg & H. C. van de Hulst, 145–152

Shenoy, S. S., Whittet, D. C. B., Chiar, J. E., Adamson, A. J., Roberge, W. G., & Hassel, G. E. 2003, *Ap. J.*, 591, 962

Smith, J. D. T., et al. 2007, *Ap. J.*, 656, 770

Smith, R. K. 2008, *Ap. J.*, 681, 343

Vaughan, S., et al. 2006, *Ap. J.*, 639, 323

Weingartner, J. C., & Draine, B. T. 2001, *Ap. J.*, 548, 296

Whittet, D. C. B., Cook, A. M., Chiar, J. E., Pendleton, Y. J., Shenoy, S. S., & Gerakines, P. A. 2009, *Ap. J.*, 695, 94

Witt, A. N., Friedmann, B. C., & Sasseen, T. P. 1997, *Ap. J.*, 481, 809

Witt, A. N., Oliveri, M. V., & Schild, R. E. 1990, *A.J.*, 99, 888

Witt, A. N., Petersohn, J. K., Bohlin, R. C., O'Connell, R. W., Roberts, M. S., Smith, A. M., & Stecher, T. P. 1992, *Ap. J. Lett.*, 395, L5

Witt, A. N., Walker, G. A. H., Bohlin, R. C., & Stecher, T. P. 1982, *Ap. J.*, 261, 492